Localized climate control in greenhouses

P.S. Booij, * **J. Sijs,** * **J.E. Fransman** **

* *TNO, Den Haag, The Netherlands*
e-mail: paul.booij@tno.nl, joris.sijs@tno.nl.
** *Delft University of Technology, Delft, The Netherlands*
e-mail: j.e.fransman@student.tudelft.nl.

Abstract: Strategies for controlling the indoor climate in greenhouses are based on a few sensors and actuators in combination with an assumption that climate variables, such as temperature, are uniform throughout the greenhouse. While this is already an improper assumption for conventional greenhouses, it especially does not hold for the new trend of growing crops at multiple layers. In addition, different temperature values are desired at the different layers, which turns out to give an uncontrollability issue with the current set of actuators. To solve this issue, fans are placed at each of the layers and an MPC strategy is employed for controlling this nonlinear MIMO system. A case study further shows that such a control strategy reduces the consumed energy of the greenhouse, while maintaining the desired temperature values.

1. INTRODUCTION

Since 2000, technical innovations within the greenhouse industry focus on the so called closed greenhouse concept: an entirely closed system allowing the grower complete control on the growing process with less energy consumed. Important parameters for growth are the spatial distribution of humidity, temperature, CO_2 and light. These parameters are controlled via a few heaters and fans and many light sources, aiming for a uniform climate throughout the greenhouse. This uniformity is important, since a greenhouse is covered with crops in the same stage of their life. However, it cannot be assumed that such a uniform distribution takes place in reality, due to natural air flow and draft through open windows. Often, fans are installed high in the greenhouse, operating at constant speed, to mix the air and thus create uniformity. Yet, in practice temperature differences up to 5 degrees are of no exception. The few sensors currently deployed in greenhouses do not provide an accurate observation of the three-dimensional climate. Moreover, the few actuation options available are not able to spatially influence the climate in a controlled manner.

Existing control systems use a simplification of the thermodynamics in a greenhouse. Nonlinear effects, such as convection at a surface and buoyancy (rise of hot air) are ignored, see for example [Bennis et al., 2008], since their corresponding physical phenomena governing the dynamics of temperature and humidity are too difficult to model and control using traditional techniques, e.g, [Caponetto et al., 2000]. On top of that, a recent trend in the greenhouses industry is to increase production by growing crops on multiple layers, rather than a single layer, as illustrated in Figure 1. Often, the stage in life of crops that are grown varies per layer, which further implies that the local climate desired for each layer is different. As such, even though it is already difficult to manage a uniform climate across one cultivation layer, in future, a control setup is desired that can create a different climate for each layer.

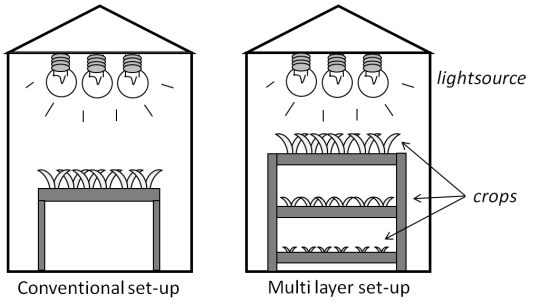

Fig. 1. Two front-views of a single section of a greenhouse. The conventional setup for growing crops involves one layer, whereas the new setup consists of multiple layers, where the life stage of crops differs per layer.

A solution to this problem is sought for along the line of networked (control) systems. Networked systems enable a setup that can measure and monitor indoor climate with high spatial resolution, which further allows for local control actions focused on targeted areas. A conceptual approach of such a networked system, for which the benefits were studied in [Speetjens et al., 2008], yields

- many small, cheap, wireless sensors provide spatial climate information with high resolution;
- multiple small, flexible actuators cooperate with existing actuators to influence the climate distribution;
- distributed control algorithms for climate optimization support ease-of-deployment.

The goal of this article is to address the second item listed above for controlling the temperature distribution of a greenhouse in multiple vertical layers. Studies related to the first and third item are found in, for example, [Camponogara et al., 2002, Speetjens et al., 2008, Witrant et al., 2009, Venkat et al., 2005]. Though solutions on the third item of distributed control show promising results, they are currently limited to linear processes. Instead, the air flow in greenhouses, which mainly results from buyonacy effects, introduces nonlinear effects in the climate model of greenhouses. Therefore, before continuing to a distributed control solution, this article studies a feasible

MIMO control strategy for a centralized system based on a nonlinear climate model. Typically, climate dynamics are captured by a CFD model (computational fluid dynamics), which is not suitable for control purposes as CFD models are computationally demanding. To solve this issue, a simplified model is presented first, which is then used in an MPC strategy for controlling the temperature values at multiple layers in the greenhouse. The case study involves the two-dimensional front view of a multi-layer greenhouse, as depicted in Figure 1. The three-dimensional case is part of future work. The greenhouse is equipped with a temperature controlled floor. This controllable actuator is extended with numerous fans to control the temperature distribution on the different layers.

2. PRELIMINARIES

$\mathbb{R}$, $\mathbb{R}_+$, $\mathbb{Z}$ and $\mathbb{Z}_+$ define the set of real numbers, non-negative real numbers, integer number and non-negative integer numbers, respectively. Further, $\mathbb{Z}_{\mathcal{C}} := \mathbb{Z} \cap \mathcal{C}$, for some $\mathcal{C} \subset \mathbb{R}$. The null-matrix and identity-matrix of corresponding dimensions are denoted as $\mathbf{0}$ and $\mathbf{I}$, respectively. For a time-varying vector $\underline{\mathrm{x}}(t) \in \mathbb{R}^n$, let us define $\underline{\mathrm{x}}[k]$ as the value of $\underline{\mathrm{x}}(t)$ at the k-th sample instant and let the matrix $\mathbf{X}[0\!:\!k] := (\underline{\mathrm{x}}[0], \underline{\mathrm{x}}[1], \cdots, \underline{\mathrm{x}}[k])$. The q-th element of a vector $\underline{\mathrm{x}} \in \mathbb{R}^n$ is denoted as $\{\underline{\mathrm{x}}\}_q$, while $\{\mathbf{A}\}_{qr}$ denotes the element of a matrix $\mathbf{A}$ in the q-th row and r-th column. The transpose and inverse (when it exists) of a matrix $\mathbf{A} \in \mathbb{R}^{n\times n}$ are denoted as $\mathbf{A}^\top$, $\mathbf{A}^{-1}$, respectively. $\mathbf{A} \succ 0$ denotes that $\mathbf{A}$ is positive definite.

3. PROBLEM FORMULATION

Let us consider the front view of a single greenhouse section, as depicted in Figure 1. The figure indicates that there are three different layers in the greenhouse at which crops are grown. Each layer desires a different temperature value for an optimal growth of the corresponding crops. Existing greenhouses control the temperature of their floor and thereby, heat the greenhouse under the assumption that crops are grown at a single layer. Such a conventional system is unable to control the different temperatures in a multi-layer setup, since heated air at the floor will directly go to the top of the greenhouse and not mix with the air in between the layers. This behavior is illustrated in a front-view of the temperature distribution in a greenhouse, see Figure 2. Note that the desired uniform temperature distribution per layer makes the control problem even more complex.

To solve this issue, numerous fans are placed for controlling the air flow in accordance with the temperature of the floor. Conventional PID control, which is most common for today's greenhouses (see [Straten and Henten, 2010]), has limited performance with the considered setup. Furthermore, it was pointed out in [Pinon et al., 2005] that actuators used in greenhouses are subject to constraints. These aspects, in combination with the following control objectives, imply that an MPC control strategy is most suitable:

- The setup requires a MIMO control strategy with constrained control actions;
- Greenhouses consume a large amount of energy but, while consumed energy is to be reduced, an increase of the production of crops is desired to maximize profits. Since these two quantities are inversely coupled an optimal trade-off should be made.
- Weather related disturbances, like clouds blocking the sun, can often be well predicted and should be anticipated in the greenhouse, as the actuators are generally too slow to surpress these disturbances using feedback only.

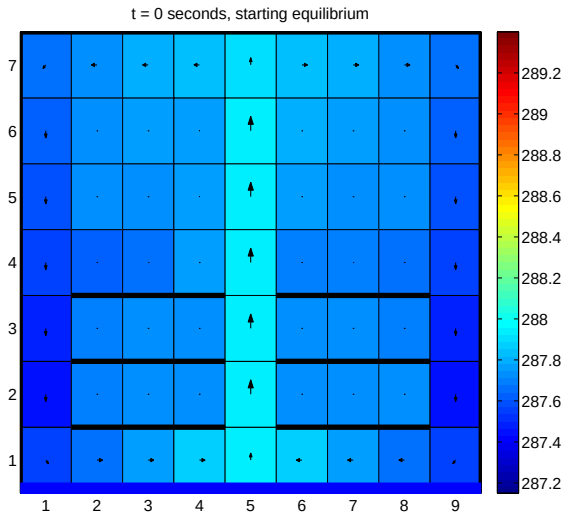

Fig. 2. Climate profile in a (simplified) multi-layer greenhouse with a temperature controlled floor. Temperature (K) is represented by color, air speed by arrows.

For the considered case study, a two-dimensional prediction model is developed, using a finite element approach. To that extent, the greenhouse is divided into rectangular cuboids, each with a grid point in its center. Each grid point $i \in \mathbb{Z}_{[1,n]}$ has a temperature $T_i \in \mathbb{R}$ and $\underline{\mathrm{T}} := (T_1\ T_2\ \cdots T_n)^\top$. Further, the air flow direction at a grid point i is the result of four flow values, each perpendicular to one of the four edges of cell i, which are collected in the vector $\underline{\mathrm{v}} \in \mathbb{R}^{4n}$. These variables define the state vector $\underline{\mathrm{x}}[k] := \left(\underline{\mathrm{T}}^\top[k]\ \underline{\mathrm{v}}^\top[k]\right)^\top$ at each k-th sample instant, for some sampling time $\tau \in \mathbb{R}_+$. Then, the state space model of the temperature distribution is characterized by some nonlinear function $f : \mathbb{R}^n \times \mathbb{R}^l \to \mathbb{R}^n$, i.e.,

$$\underline{\mathrm{x}}[k+1] = f(\underline{\mathrm{x}}[k], \underline{\mathrm{u}}[k]). \tag{1}$$

Control actions that regulate the fans and the floor temperature are represented by $\underline{\mathrm{u}}[k] \in \mathbb{R}^l$. Further, let the state and control values be bounded by $\underline{\mathrm{x}}[k] \in \mathcal{X} \subseteq \mathbb{R}^n$ and $\underline{\mathrm{u}}[k] \in \mathcal{U} \subseteq \mathbb{R}^l$, for all $k \in \mathbb{Z}_+$. For clarity of the control strategy, let us assume that current temperature and air flow distributions of the greenhouse, i.e., $\underline{\mathrm{x}}[k]$, are fully available, for example, via a state estimation method.

The goal is to develop an MPC algorithm for controlling the temperature values of the greenhouse at the different layers, while simultaneously minimizing energy consumed by the actuators. To that extent, a derivation of the state space model in (1) is presented, next. The derivation provides a simplification of the temperature and air flow relations, driving heat transport by conduction and convection. Subsequently, the employed MPC is developed, followed by a two-dimensional case study for controlling the temperature profile in the considered greenhouse.

4. CLIMATE MODEL

This section presents the climate model that will be used for simulation and for prediction in the MPC algorithm. A detailed account on the derivation of the model does not suit the focus of this article. Instead, a description is given of the three main drivers that determine the temperature distribution within a greenhouse, i.e.,

- heat conduction in air;
- heat convection at a surface;
- heat transport through air flow (buoyancy and fans).

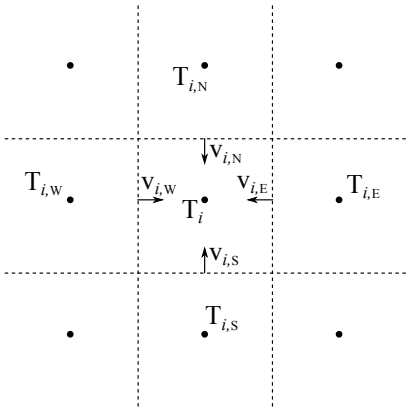

Fig. 3. An illustration of the temperature and air speed variables of cell i with respect to its neighboring cells, i.e., denoted as north, east, south and west.

Let the two-dimensional area be divided into n cells, according to Figure 2. Each cell i has a temperature $T_i[k]$, density $\rho_i[k]$ and four air speed values corresponding to the edges of cell i, i.e., $v_{i,\text{W}}[k]$, $v_{i,\text{E}}[k]$, $v_{i,\text{S}}[k]$ and $v_{i,\text{N}}[k]$, see also Figure 3. Note that the temperatures in the neighboring cells that surround the i-th cell are denoted as $T_{i,\text{W}}[k]$ (west), $T_{i,\text{E}}[k]$ (east), $T_{i,\text{S}}[k]$ (south) and $T_{i,\text{N}}[k]$ (north).

Remark 4.1. The fact that air flow is continuous at edges implies that if cell j is a neighbor of cell i, such that $T_{i,\text{W}} = T_j$, then $v_{i,\text{W}}[k] \equiv -v_{j,\text{E}}[k]$ holds. Further, boundary conditions impose that if the edge of cell i is characterized by a surface, i.e., walls, ceiling, floor or layers, the air speed perpendicular to that surface is 0.

Let us continue with a characterization of the process model $f(\cdot,\cdot)$, for which it is sufficient to introduce the dynamic behavior of each temperature value $T_i[k+1]$ as a function of its surrounding variables at the k-th sample instant. Further, let the density of cell i be given as

$$\rho_i[k] = \frac{P}{R \cdot T_i[k]}, \tag{2}$$

where R is the *gas constant* and P is the pressure in the greenhouse. Then, the results of [Patankar, 1980] imply that the expression to determine the next temperature value of cell i, is given by

$$T_i[k+1] = \frac{1}{a[k]}\Big(a_0[k]T_i[k] + \sum_{q\in\{\text{W,E,S,N}\}} a_{i,q}[k]T_{i,q}[k]\Big), \tag{3}$$

$$a[k] = a_0[k] + \sum_{q\in\{\text{W,E,S,N}\}} a_{i,q}[k], \quad a_0[k] = \frac{\rho_i[k]c_pV_i}{\tau}.$$

Note that in (3), $\sum_{q\in\{\text{W,E,S,N}\}} a_{i,q}[k]$ is a short notation for $a_{i,\text{W}}[k]+a_{i,\text{E}}[k]+a_{i,\text{S}}[k]+a_{i,\text{N}}[k]$, with a similar concept for the sum $\sum_{q\in\{\text{W,E,S,N}\}} a_{i,q}[k]T_{i,q}[k]$. The parameters c_p and V_i are the *specific heat* (capacity) of air and the volume of cell i, respectively. Further, the scalar variables $a_{i,q} \in \mathbb{R}_+$, for all $q \in \{\text{W,E,S,N}\}$, determine the influence of neighboring temperature values on T_i. They are characterized by a "conduction/convection" term $D_{i,q} \in \mathbb{R}_+$ and a mass flow term $F_{i,q} \in \mathbb{R}_+$ that depends on the air speed, for all $q \in \{\text{W,E,S,N}\}$, i.e.,

$$a_{i,q}[k] = D_{i,q}[k] + \max\{F_{i,q}[k], 0\}, \quad \forall q \in \{\text{W,E,S,N}\}. \tag{4}$$

The value of $D_{i,q}[k] \sim \beta_{air}$ is proportional to the *heat conductivity* of air $\beta_{air} \in \mathbb{R}_+$, if the corresponding neighbor is another cell. In case cell i is bordered by a surface, then $D_{i,q}[k] \sim h_{i,q}[k]$ is proportional to the *convection coefficient* $h_{i,q}[k] \in \mathbb{R}$. This coefficient has nonlinear, nonconvex and discontinuous properties depending on, for example, the "Nusselt number", turbulent or laminar air behavior, the distance to the surface, the air flow parallel to the surface and the difference in temperature values. Note that the controlled floor temperature influences the temperature in the greenhouse according to such a convection coefficient. The interested reader is referred to [Incropera et al., 2005] for more details. Here, let us continue with the mass flow term $F_{i,q}$ depending on the corresponding air speed, see [Patankar, 1980], i.e.,

$$\begin{aligned} F_{i,q}[k] &= \rho_i[k]c_pH_i \cdot v_{i,q}[k], \quad \forall q \in \{\text{W,E}\}, \\ F_{i,q}[k] &= \rho_i[k]c_pW_i \cdot v_{i,q}[k], \quad \forall q \in \{\text{S,N}\}, \end{aligned} \tag{5}$$

where $H_i \in \mathbb{R}_+$ is the height of cell i, while $W_i \in \mathbb{R}_i$ denotes its width. The remaining variables to complete the process model are the four air speed values of cell i at the different edges $q \in \{\text{W,E,S,N}\}$, which are derived, next.

Recall that $\underline{\text{v}}$ denotes the collection of all air speed values in the greenhouse at the corresponding sample instant, i.e.,

$$\underline{\text{v}} = (v_{1,\text{N}}\ v_{1,\text{E}}\ v_{1,\text{S}}\ v_{1,\text{W}}\ \cdots\ v_{n,\text{N}}\ v_{n,\text{E}}\ v_{n,\text{S}}\ v_{n,\text{W}})^\top$$

Then, the expression to determine $\underline{\text{v}}[k+1]$ is introduced via a linear state space representation, yielding

$$\underline{\text{v}}[k+1] := \mathbf{A}\underline{\text{v}}[k] + \mathbf{B}_\rho \underline{\text{u}}_\rho[k] + \mathbf{B}_f \underline{\text{u}}_f[k]. \tag{6}$$

The variables $\underline{\text{u}}_\rho[k] \in \mathbb{R}^n$ and $\underline{\text{u}}_f[k] \in \mathbb{R}^{l-1}$ denote the sources of the air flow, i.e., the buoyancy speed and controlled fans, respectively. Each of these sources acts directly on a particular air speed, due to which the elements of $\mathbf{B}_\rho \in \mathbb{R}^{4n\times n}$ and $\mathbf{B}_f \in \mathbb{R}^{4n\times l-1}$ are either equal to 0 or 1. Note that the control action $\underline{\text{u}}[k] \in \mathbb{R}^l$ thus consists of the controlled floor temperature, denoted as $T_{floor}[k] \in \mathbb{R}$, and of the above controlled fans $\underline{\text{u}}_f[k]$. To characterize the effect of the buoyancy speed, let us define $u_{i,\rho}[k] \in \mathbb{R}^n$ as a speed additional to the northern air speed of each cell i, i.e., $v_{i,\text{N}}[k]$. As such, it follows that $\underline{\text{u}}_\rho[k] := (u_{1,\rho}[k] \cdots u_{n,\rho}[k])^\top$. The buoyancy speed is modeled as air speed in the northern direction that is either negative, for heated air that will go up, or positive, for cold air that tends to go down. Further, the force driving the buoyancy speed depends on the average density in cell i with respect to the average densities of the cells on the West and East, proportional to the gravitational constant g, i.e.,

$$u_{i,\rho}[k] : = g\left(1 - \frac{\frac{1}{2}(\rho_{i,\text{W}}[k] + \rho_{i,\text{E}})[k]}{\rho_i[k]}\right), \tag{7}$$

The remaining matrix $\mathbf{A} \in \mathbb{R}^{4n\times 4n}$ in (6) governs the propagation of the sources into a consistent flow field.

Physics dictate that a flow field should obey the laws of mass conservation, energy conservation and momentum conservation. For more information on these laws, the reader is referred to [Patankar, 1980]. The coefficients of $\mathbf{A}$ are chosen inspired by conservation of momentum, i.e. air flow wants to propagate in its original direction, unless hindered by surfaces or colliding flow. This also satisfies the boundary conditions from Remark 4.1. The resulting matrix $\mathbf{A}$ obeys the law of mass conservation, but introduces a small error regarding the law of energy conservation. In the results of Section 6, some energy was dissipated in the model (< 2.5 J/s).

5. MODEL PREDICTIVE CONTROL

A MIMO controller is constructed that calculates the actuator input matrix $\mathbf{U} = (\underline{u}[0], \underline{u}[1], \cdots)$, in order to achieve a desired climate profile, with minimal energy. This can be formulated as the minimization of a quadratic objective function J, according to

$$\min_{\mathbf{U}} J = \sum_{k=0}^{\infty} \underline{\epsilon}[k]^\top \mathbf{Q} \underline{\epsilon}[k] + \underline{u}[k]^\top \mathbf{R} \underline{u}[k], \tag{8}$$

where $\underline{\epsilon}[k] = \underline{T}[k] - \underline{\sigma}[k] \in \mathbb{R}^n$ is a vector containing the temperature tracking errors with respect to setpoints $\underline{\sigma}[k]$, $\mathbf{Q} \succ 0 \in \mathbb{R}^{n \times n}$ defines the costs of these tracking errors and $\mathbf{R} \succ 0 \in \mathbb{R}^{l \times l}$ defines the costs of the actuation.

The minimization in (8) is approximated using a receding horizon approach. At each time instant k_c, corresponding with controller sampling time $\tau_c > \tau$, the actuation matrix $\tilde{\mathbf{U}}[k_c] = (\tilde{\underline{u}}[0], \cdots, \tilde{\underline{u}}[H_c - 1]) \in \mathbb{R}^{l \times H_c}$ is calculated, minimizing

$$\begin{aligned} \min_{\tilde{\mathbf{U}}} J = & \sum_{\kappa=k_c}^{k_c+H_p-1} \underline{\epsilon}[\kappa]^\top \mathbf{Q} \underline{\epsilon}[\kappa] + \sum_{\kappa=0}^{H_c-1} \tilde{\underline{u}}[\kappa]^\top \mathbf{R} \tilde{\underline{u}}[\kappa] \\ & + (H_p - H_c) \tilde{\underline{u}}[H_c - 1] \mathbf{R} \tilde{\underline{u}}[H_c - 1]. \end{aligned} \tag{9}$$

Here, H_c is the control horizon and $H_p \geq H_c$ is the prediction horizon. If $H_p > H_c$, the inputs $\tilde{\underline{u}}[H_c - 1]$ are maintained during the remaining $H_p - H_c$ controller sampling intervals. After each optimization, $\underline{u}[k_c] = \tilde{\underline{u}}[0]$ is applied to the system. After τ_c seconds, the entire process is repeated.

Using the model described in Section 4, predictions of the temperature tracking error $\epsilon[\kappa]$, for all $\kappa \in \mathbb{Z}_{[k_c \; k_c+H_p-1]}$ as a function of $\tilde{\mathbf{U}}[k_c]$ can be made. Note that the model is highly nonlinear and discontinuous, which means that gradient based solvers cannot be used to perform the minimization in (9), as these would either loose stability due to discontinuity, or converge to a local minimum due to non-convexity of the prediction model. Therefore, we use MIDACO [1], [Schlüter et al., 2009], a derivative free solver that aims to find the global minimum.

The MIDACO solver is based on ant colony optimization and was especially designed for constrained mixed integer nonlinear optimization problems, though it can also handle other problems, such as the continuous unconstrained nonlinear problem in (9). The solver will escape local minima, though it might need many function evaluations to do so. It is impossible to know beforehand how many iterations are necessary and therefore how much time is needed for the global optimum to be reached. From experience with the problem in this paper, it ranges between hundreds and thousands iterations, depending on the number op optimization variables. Fortunately, MIDACO offers extensive parallelization options, significantly reducing the computation time. The MIDACO solver also allows for a 'warm start', meaning that an initial guess of the optimal actuation trajectory can be provided as a starting point for the solver [Schlüter et al., 2009]. This way, part of the previously calculated actuator input trajectory can be provided as a starting point for the optimization in the next controller time step, reducing the optimizer's time till convergence. Specifically, $(\tilde{\mathbf{U}}[1 : H_c - 1], \; 0.5\tilde{\underline{u}}[H_c - 1])$ of the optimized $\tilde{\mathbf{U}}[k_c - 1]$ is provided as starting point for the optimization at time k_c.

[1] http://www.midaco-solver.com

6. GREENHOUSE CASE STUDY

The aim is to create a climate profile such that the temperature in the lower layers is higher than in the middle and upper layers, using minimal energy. This relates to the situation in which the lower layers are used for germination, the middle layers for young plants and the top layer for adult plants. The allowable temperature range is smallest for the lowest layer and increases as the plant grows older. The adult plants in the top layer can handle the largest temperature variations. This is captured by choosing $\underline{\sigma}$ and $\mathbf{Q}$ such that the setpoint for the cells in the lower layers is 288.65 K, with related tracking error costs of 0.26. For the cells in the middle layers, the setpoint is 288.15 K with corresponding tracking error costs of 0.24. The outside temperature is 283.15 K.

The choice of parameters τ_c, H_p, H_c in (9) represents a trade-off between accurately approximating (8) and computational feasibility. A small value for controller sampling time τ_c will allow the controller to track the setpoints accurately and without overshoot, but comes at a price of having only a time budget of τ_c seconds to perform the optimization when operating in real-time. A large prediction horizon H_p needs more computation for each iteration in the optimization, but results in a smoother controller. Prediction horizon H_p should at least be taken large enough to make the effects of the floor heater observable in (9). Finally, A large control horizon H_c will give a more accurate calculation of the optimal $\underline{u}[k_c] = \tilde{\underline{u}}[0]$ which is to be injected into the system. However, it is a multiplier to the amount of optimization variables and therefore severly influences the required computation time. With aforementioned taken into consideration, we have chosen $\tau_c = 60$ seconds, $H_p = 9$, (540 seconds) and $H_c = 2$, (120 seconds), which results in 10 optimization variables and a computation time of approximately 0.59 s for 6 parallel function evaluations on a 6-core Intel(R) Core(TM) i7-3960X CPU.

Figure 4 depicts the result of using only floor heating to warm up the greenhouse, with $\tilde{\underline{u}}[k_c] = \tilde{u}_{floor}[k_c]$ the input to the floor heating which is bounded by $0 \leq \tilde{u}_{floor}[k_c] \leq 10000$ Watts and has associated costs given by $\mathbf{R} = 10^{-9}$. Clearly, with such a setup it is infeasible to create warmer climates at the bottom of the greenhouse and colder climates above. Instead, buoyancy forces accelarate the

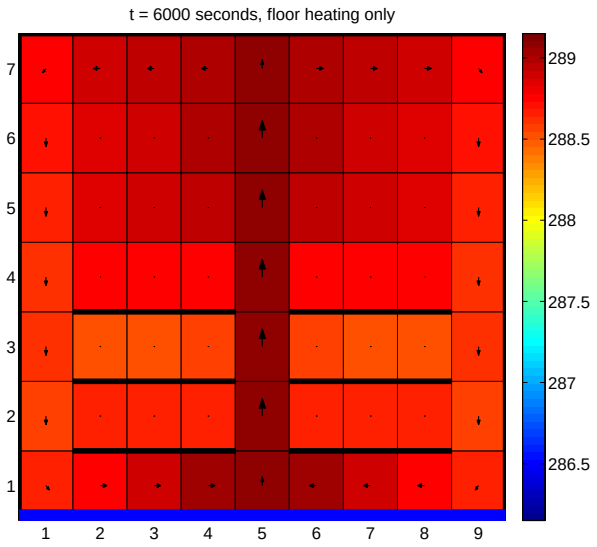

(a) Climate profile after 6000 seconds of control with floor heating. Temperature (K) is represented by color, air speed by arrows.

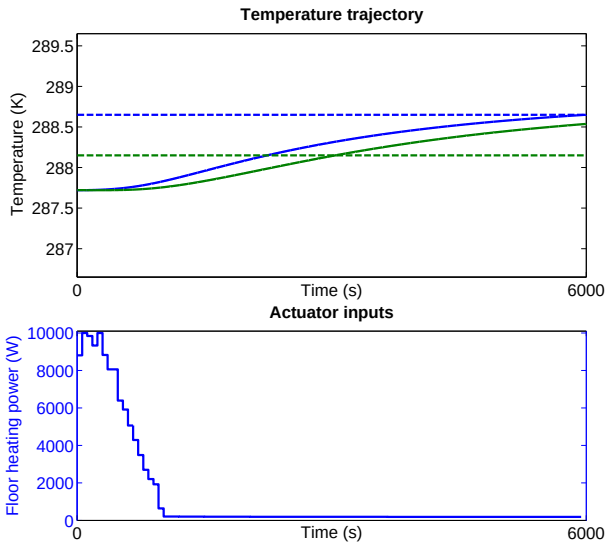

(b) Temperatures in lower (blue) and middle (green) layer, with corresponding setpoints (dotted). Actuation of floor heating.

Fig. 4. Results of using MPC on floor heating only to create different climate conditions per layer. The contruction of the layers prevents warm air from entering. Instead, the greenhouse is slowly heated from top to bottom.

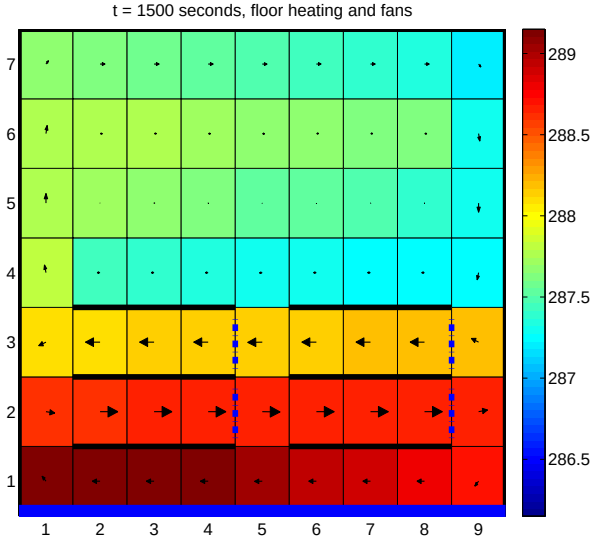

(a) Climate profile after 1500 seconds of control with floor heating and fans (blue dotted lines). Temperature (K) is represented by color, air speed by arrows.

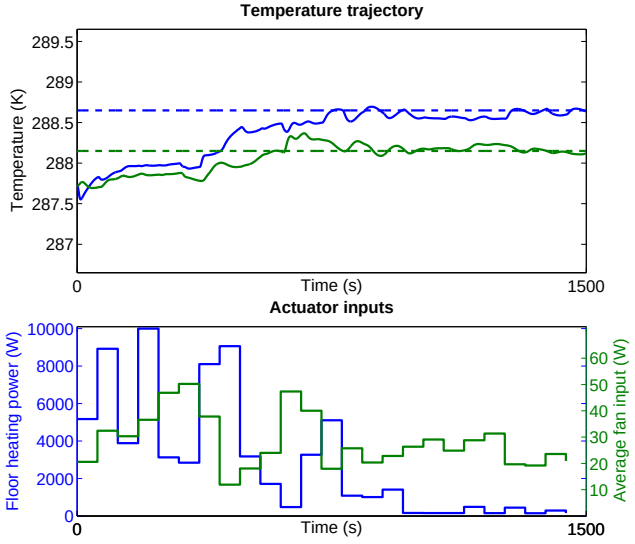

(b) Temperatures in lower (blue) and middle (green) layer, with corresponding setpoints (dotted). Actuation of floor heating (blue) and average of 4 fans (green).

Fig. 5. Results of using MPC on floor heating and fans to create different climate conditions per layer. Warm air is routed through the layers and short circuited back to the floor, warming only the relevant parts of the greenhouse.

warm air upwards and most of the energy ends up high in the greenhouse where no plants are present. Moreover, due to the construction of the multi-layer cultivation setup, natural air flow can hardly gets into the layers. In practice, the plants in the layers further inhibit airflow. As a result, heat transport near the plants is dominated by conduction, instead of convection, which is orders of magnitude slower. In some cases it might even be too slow to compensate for the heat a plant drains from its surroundings to support its vaporization process (not modelled here). In Figure 4b, it can be seen that it takes approximately 6000 seconds to obtain the desired temperature in the lowest layer, with a too high temperature in the middle layer.

We propose to overcome these problems by adding four fans, as depicted in Figure 5a by the dotted blue lines. By properly controlling the floor heating and the fans, the warmth rising from the floor should be routed through the layers. Preferably, the air is then rerouted back to the floor to be reheated, instead of ending up in the top of the greenhouse. The actuator input vector is extended to $\underline{\mathrm{u}}[k_c] = \left(\tilde{u}_{floor}[k_c], \underline{\tilde{\mathrm{u}}}^{\top}_{fans}[k_c]\right)^{\top}$ with fan input boundaries $\underline{0} \leq \underline{\tilde{\mathrm{u}}}_{fans}[k_c] \leq \underline{72}$ Watts per fan, which corresponds to a maximum induced airflow of 0.4 m/s per fan. Note that the fans in the bottom layer blow to the right, while the fans in the middle layer blow to the left. The related costs for the actuation is provided by $\mathbf{R} = \mathrm{diag}\{\left(10^{-9}, 0.025, 0.025, 0.025, 0.025\right)\}$.

The results of this setup are shown in Figure 5. In Figure 5a, it can clearly be seen that the heated air

is indeed routed though the layers and returned to the floor to be reheated. Due to this shortcut, hot air hardly infiltrates the top half of the greenhouse, which actually cools down during the 1500 seconds simulation due to the cold outside. The right figure shows that the temperatures in the layers assume there setpoint values after about 1000 seconds, after which the system enters a certain steady state. This steady state solution is an instable thermal situation, with warm air below and cool air above. This situation can only be maintained using the fans.
Comparing to the conventional setup of using only floor heating with the setup containing additional fans, the latter is able to reach all desired setpoints 6 times faster than the conventional setup, which can only satisfy one setpoint. The setup with fans uses 39.7% less energy in reaching these setpoints. More importantly, in maintaining the desired temperature profile, 19.8% energy is saved, by not heating up the upper half of the greenhouse.

While the model described in Section 4 is able to perform 150 times faster than real-time for the given system (using only one core of the CPU), the time needed for the solver to approximate the global optimum still far exceeds the time budget of $\tau_c = 60$ s that is available in real-time operation. The results in Figure 4 are obtained using a time budget of 1800 seconds for each optimization. Yet, even when stopping the optimizer after τ_c seconds and using the intermediate results, the controller is stil able to perform satisfactory, all be it in a less smooth fashion. Figure 6 shows the results for the controller when operating in real-time. Compared to the results in Figure 5, it can be seen that the 'suboptimal' real-time controller needs more time to achieve the same steady state solution. In the process of heating up, more heat escapes the optimal route and leaks to the top of the greenhouse.
Using the realtime controller, all setpoints are still achieved 4 times faster than in the conventional setup. The energy savings in reaching the setpoints are significantly lower than in the controller from Figure 5, yet still 20.5%. Maintaining the setpoint, especially in the presence of disturbances, will also be less efficient, but in this example energy savings of 9.8% are still achieved.

7. DISCUSSION AND CONCLUSIONS

The presented results show that it is possible to create multiple climates at different layers in a greenhouse, while saving a significant amount of energy. This has been done by deploying fans and controlling them using an MPC approach with a physical prediction model. It should be noted that in this study, the used model is still fairly coarse and only two-dimensional. Moreover, the same model was used for simulation of the greenhouse and prediction in the controller, without presence of unknown disturbances and with the assumption of having optimal state estimation. With this in mind, it should not be expected that the presented energy saving in the order of 40% can actually be achieved in practice. However, given that the model includes all relevant heat transport processes, this first attempt of localized climate control validates further investigation into the topic.
Future work includes refinement of the model, tuning of solver parameters to increase convergence speed and experimenting in a small scale greenhouse (22 m^3).

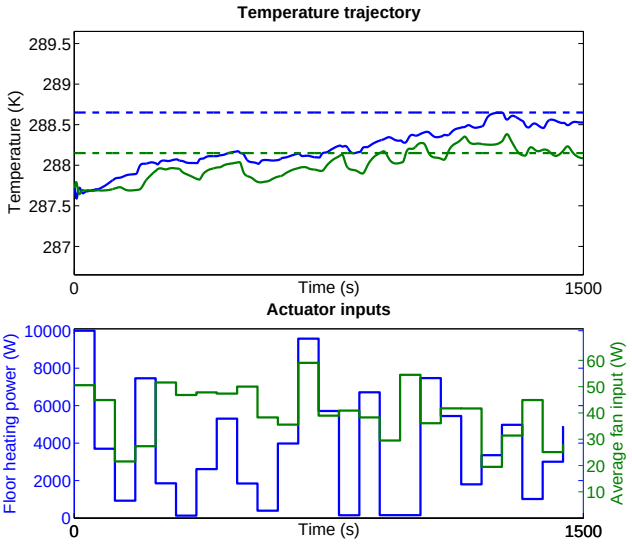

Fig. 6. Temperatures in lower (blue) and middle (green) layer, with corresponding setpoints (dotted). Actuation of floor heating (blue) and average of 4 fans (green), resulting from real-time controller.

REFERENCES

N. Bennis, J. Duplaix, G. Enéa, M. Haloua, and H. Youlal. Greenhouse climate modelling and robust control. *Computers and electronics in agriculture*, 61(2):96–107, 2008.

E. Camponogara, D. Jia, B.H. Krogh, and S. Talukdar. Distributed model predictive control. *Control Systems, IEEE*, 22(1):44–52, 2002.

R. Caponetto, L. Fortuna, G. Nunnari, L. Occhipinti, and M.G. Xibilia. Soft computing for greenhouse climate control. *Fuzzy Systems, IEEE Trans. on*, 8(6):753–760, 2000.

F. Incropera, D. DeWitt, and T. Bergman. *Fundamentals of heat and mass transfer, 5-th edition*. John Wiley & Sons, 2005.

S. Patankar. *Numerical heat transfer and fluid flow*. Hemisphere Publishing Corporation, 1980.

S. Pinon, E.F. Camacho, B. Kuchen, and M. Peña. Constrained predictive control of a greenhouse. *Computers and Electronics in Agriculture*, 49(3):317–329, 2005.

M. Schlüter, J. Egea, L.T. Antelo, A. Alonso, and J.R. Banga. An extended ant colony optimization algorithm for integrated process and control system design. *Industrial & Engineering Chemistry*, 48(14):6723–6738, 2009.

S.L. Speetjens, H.J.J. Janssen, G. Van Straten, T.H. Gieling, and J.D. Stigter. Methodic design of a measurement and control system for climate control in horticulture. *Computers and Electronics in Agriculture*, 64(2):162–172, 2008.

G. Straten and E.J. Henten. Optimal greenhouse cultivation control: survey and perspectives. *Conference paper Narcis*, 2010.

A.N. Venkat, J.B. Rawlings, and S.J. Wright. Stability and optimality of distributed model predictive control. In *Decision and Control, European Control Conf. CDC-ECC '05. 44th IEEE Conf. on*, pages 6680–6685, 2005.

E. Witrant, S. Mocanu, and O. Sename. A hybrid model and mimo control for intelligent buildings temperature regulation over WSN. In *Proc. of the 8th IFAC Workshop on Time Delay Systems*, Sinaia, Romania, 2009.